



24th COBEM - 2017



24th ABCM International Congress of Mechanical Engineering
December 3-8, 2017, Curitiba, PR, Brazil

COBEM-2017- 1955

NUMERICAL AND EXPERIMENTAL ANALYSES OF HEAT TRANSFER BY NATURAL CONVECTION ON FLAT INCLINED PLATES

João Gabriel Gomes de Oliveira

Eugênia Cornils da Silva

Taygoara Felamingo de Oliveira

Antonio Cesar Pinho Brasil Junior

University of Brasília, Faculty of Technology, Laboratory of Energy and Environment, CEP. 70910-900 – Brasília, DF – Brazil
joao_unb_enm@hotmail.com; eugeniacornils@yahoo.com.br; taygoara@unb.br; brasiljr@unb.br

Abstract. *The steady-state natural convection heat transfer from flat inclined plates for laminar flow is numerically investigated. The numerical modeling approach is validated by an experimental study in a natural convection chamber and by comparing the inclined heated flat plate results with the available correlations. The convective heat transfer coefficient of the heated plate is obtained from finite volume computational fluid dynamics simulations. The 2D and 3D domains were considered in order to evaluate the contributions of the three-dimensional effects. For the inclination angles 10°, 15°, 20°, 25°, 30°, 35°, 40°, 45°, 50°, 55° and 60° from the horizontal position, the extent of validity of the obtained vertical correlation is investigated by modifying the Rayleigh number with the sine of the inclination angle. The results of convective heat transfer coefficient are represented in the relation of average Nusselt and Rayleigh numbers. An appropriate numerical model approach was developed. The results of the new model agree well with the experiment and available correlations.*

Keywords: *natural convection, flat inclined plate, convective heat transfer coefficient, CFD simulations.*

1. INTRODUCTION

Several applications involving the natural convection heat transfer on inclined surfaces are found in practical engineering problems. In the literature, many reports have quantified the angular dependence of the heat transfer coefficient for different inclined geometries (Vliet, 1969; Fujii and Imura, 1972; Azevedo and Sparrow, 1985; Souza *et al.*, 1993; Tari and Mehrtash, 2013; Jubayer *et al.*, 2016; Pinheiro *et al.*, 2016).

Numerical simulations were used to investigate the influence of the inclination angle of inclination (ϕ) on the heat transfer coefficient for a flat inclined plate that was submitted to natural convection heat transfer. In addition to the inclination, one other parameter was varied during the numerical simulation expressed by the Rayleigh number (Ra). The plate constant temperature was set as 25°C, 30°C, 40°C, 50°C, 60°C, 70°C and 80°C.

The numerical configuration reproduces an experimental setup, which results were used to validate the simulation method. The experiments were performed in the air ($Pr = 0,7$). The Churchill and Chu's correlation (Churchill and Chu, 1975) for the laminar regime was also used in order to check the accuracy of numerical computations.

Despite accurate correlations being available for bi-dimensional natural convection on inclined flat plates, 3D phenomena occurring when plate's aspect ratio is about unity are still remains not well understood and potentially may influence the convection heat transfer coefficient in significant ways.

The aim of the present work is to study the dependence of the heat transfer coefficient on the aspect ratio of an inclined flat plate around which thermal buoyancy driven flow occurs. The formation of three-dimensional flow structures on the upper face of the flat inclined plate is investigated.

2. COMPUTATIONAL PROCEDURE

The software ANSYS Workbench™ was used to perform Computational Fluid Dynamics (CFD) analysis for laminar flow, considering the two and three-dimensional domains composed of an inclined plate. Steady-state solutions were obtained for air flow over the plate. The flow was incompressible and Buoyancy was modeled using the Boussinesq approximation in which the forces are modeled as source terms in the momentum equations.

Nomenclature

C_p	specific heat	[J/kg-K]
g	acceleration of gravity	[m/s ²]
\bar{h}	average heat transfer coefficient	[W/m ² -K]
k	thermal conductivity of fluid (air)	[W/m-K]
L	characteristic length	[m]
\overline{Nu}_L	average Nusselt number based on L	[-]
p	pressure	[atm]
Pr	Prandtl number	[-]
Ra	Rayleigh number	[-]
T	temperature	[°C]
T_∞	ambient temperature	[°C]
T_f	film temperature	[°C]
T_w	wall temperature	[°C]
\bar{u}	velocities in x, y and z directions	[m/s]
<i>Greek symbols</i>		
α	thermal diffusivity	[m ² /s]
β	volumetric thermal expansion coefficient	[1/K]
ν	kinematic viscosity	[kg/m ³]
ρ	density	[m ² /s]
ϕ	angle of inclination with respect to horizontal position	[degrees]

The continuity, Eq. (1), momentum, Eq. (2), and thermal energy, Eq. (3), equations with their boundary conditions were solved with ANSYS Fluent R17.0 and ANSYS CFX R16.1 for the 2D and 3D domains, respectively.

$$\nabla \cdot \bar{u} = 0 \quad (1)$$

$$\rho \frac{D\bar{u}}{Dt} = -\nabla p + \mu \nabla^2 \bar{u} + \rho g \beta (T - T_\infty) \quad (2)$$

$$\frac{DT}{Dt} = \alpha \nabla^2 T \quad (3)$$

In these equations the velocity and temperature fields were obtained from the Reynolds-Averaged Navier-Stokes (RANS) calculations.

2.1 Computational domain

The flow domain dimensions were set with reference to the plate characteristic length, $L = 10$ cm. Figure 1 shows the front and side views of the 3D computational domain. The 2D domain dimensions were the same of the side view of the 3D domain.

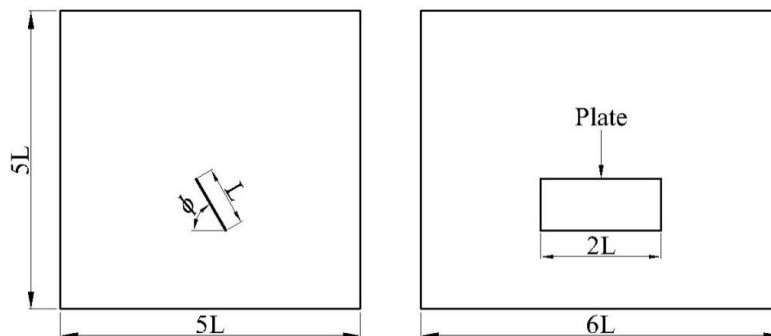


Figure 1: The dimension of 3D computational domain.

2.2 Computational mesh

A mesh study was carried out using the numerical simulations results for the average heat transfer coefficient on the surfaces of the flat plate. The refinement of 2D and 3D meshes was performed by decreasing the size of the element until there were no significant changes in the average heat transfer coefficient. The 2D mesh contains 18.531 nodes, 18.229 tetrahedral and prismatic elements, Fig. 2(a). The 3D mesh contains 942.963 nodes and 5.124.469 tetrahedral elements, Fig. 3(b).

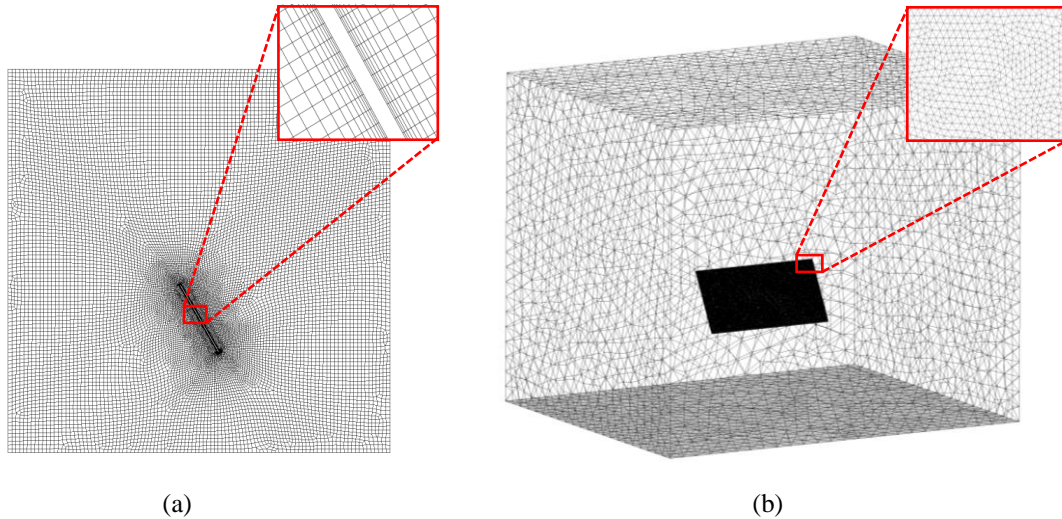


Figure 2: The view of computational mesh. (a) 2D; (b) 3D.

2.3 Boundary conditions

For the momentum boundary conditions, the plate surfaces and the bottom of the domain were treated as no slip walls. A fixed uniform zero gauge and relative pressure boundary were used at the lateral and top of the 2D and 3D domains, respectively, Fig. 3. For the thermal boundary conditions, an ambient temperature of 22°C was chosen. Therefore the lateral, bottom and top of the domain were initialized with 22°C temperature. The plate surfaces constant temperature was set as 25°C, 30°C, 40°C, 50°C, 60°C, 70°C and 80°C for each simulation. The angle of inclination was set as 10°, 15°, 20°, 25°, 30°, 35°, 40°, 45°, 50°, 55° and 60° with respect to horizontal position for each plate temperature.

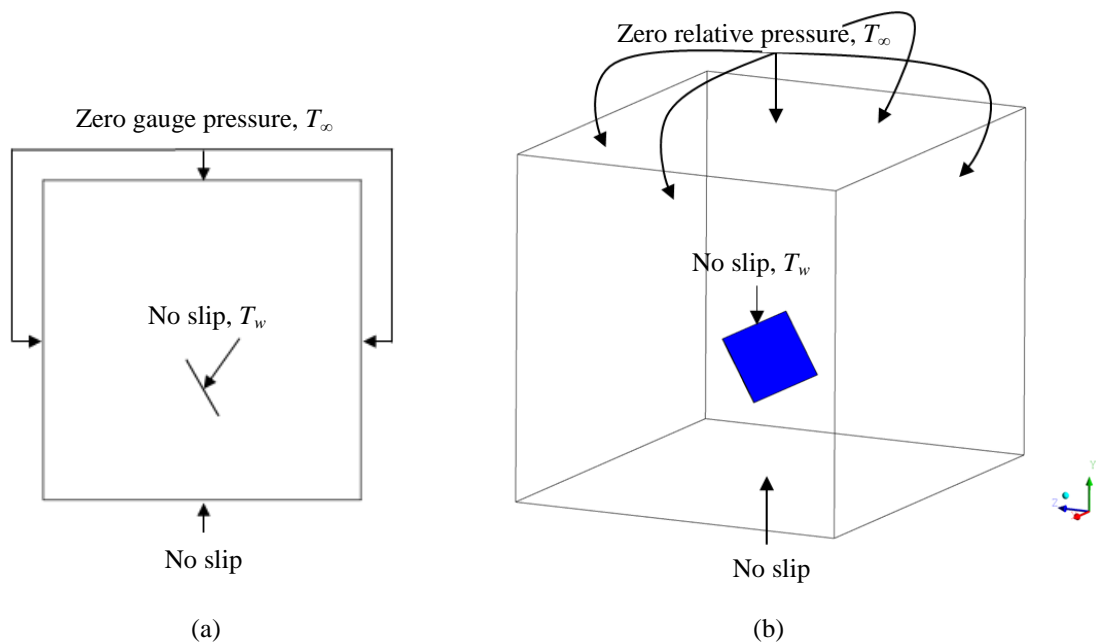


Figure 3: Boundary conditions. (a) 2D; (b) 3D.

2.4 Vertical model validation

The simulation results were validated through comparison with Churchill and Chu's relation for a laminar flow for a vertical plate, Eq. (4). The Rayleigh number (Ra) was defined relying on the plate characteristic length L , Eq. (5), in which g is the gravitational acceleration, T_w and T_∞ are the plate surfaces and ambient temperatures, respectively. All properties of air ρ , ν , β and Pr , Eq. (6), were evaluated in the film temperature, Eq. (7).

$$\overline{Nu_L} = 0.68 + \frac{0.670 Ra^{1/4}}{\left[1 + (0.492 / Pr)^{9/16}\right]^{4/9}} \quad (4)$$

$$Ra = \frac{g \beta L^3 (T_w - T_\infty)}{\nu^2} \quad (5)$$

$$Pr = \frac{\mu C_p}{k} \quad (6)$$

$$T_f = (T_w + T_\infty) / 2 \quad (7)$$

The average heat transfer coefficients (\bar{h}) were obtained for plate surfaces (upward and downward) for 2D and 3D domains. The plate temperature was varied by 5°C from 25°C to 80°C. The empirical relation, Eq. (8), was used to obtain the average of Nusselt number ($\overline{Nu_L}$) for simulations. The comparative results between the $\overline{Nu_L}$ per Ra for numerical simulations (2D and 3D) and Churchill and Chu's relation are shown in Fig. (4). The agreement of the results is good indicating a suitable modeling approach. This model was used to perform the numerical simulations for the inclined plate.

$$\overline{Nu_L} = \frac{\bar{h} \cdot L}{k} \quad (8)$$

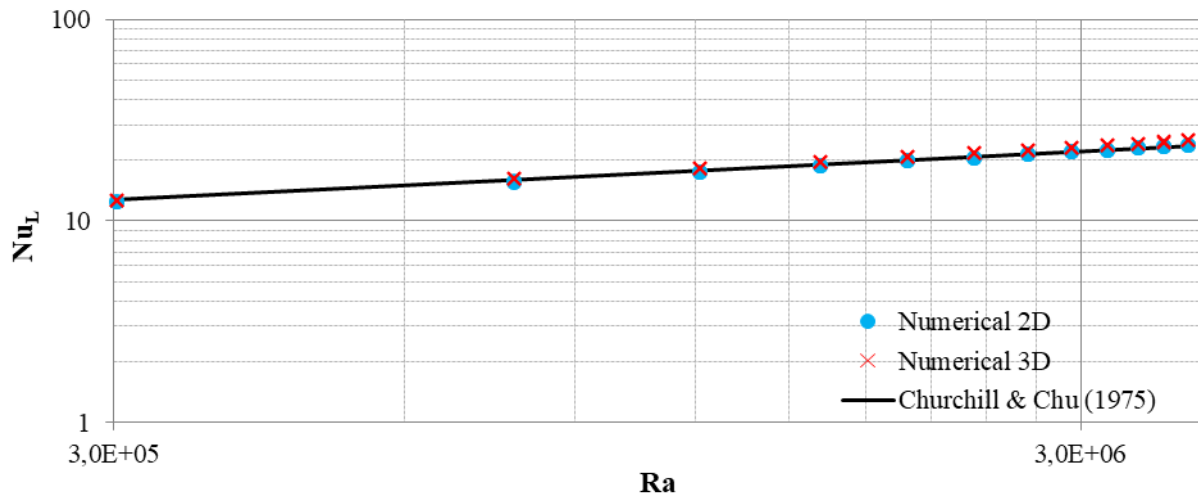


Figure 4: Vertical heated flat plate, $\phi = 90^\circ$.

3. EXPERIMENTAL PROCEDURE

Figure 5 shows an experimental setup used. Two stainless steel plates of 0,2 m (length) \times 0,1 m (width) \times 0,001 m (thickness) were assembled together with holding acrylic support allowing inclination changes. The inclination angle of the heated surface can vary from 20° to 60° with respect to the vertical position by a manual locking, Fig. 5(a), and the setup was placed into a closed chamber, Fig. 5(b). The plate's temperature was kept constant by a flexible electric heater connected to an electric source.

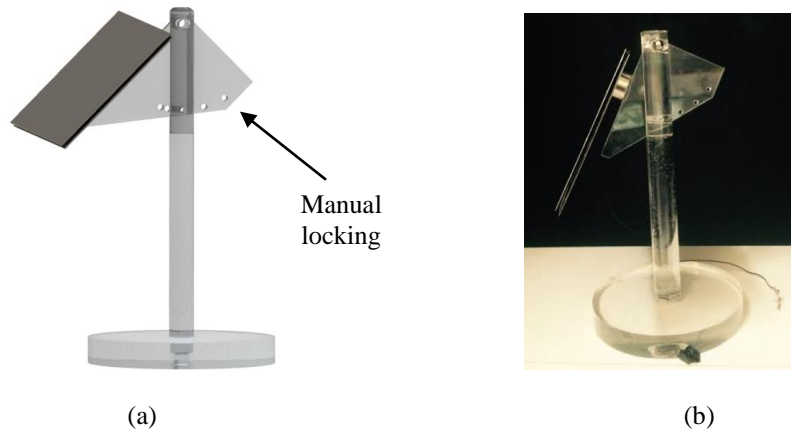


Figure 5: Experimental setup. (a) Schematic view; (b) Placed into a closed chamber.

Two differential type (J-K) thermocouples were positioned on the top and bottom surfaces of the module. Then, a temperature type DS18B20 sensor was attached near to the wall to measure the ambient temperature and to calculate the temperature difference ($T_w - T_\infty$). The current and voltage data were acquired through sensors connected to the voltage source and the Arduino UNO.

The polyimide film insulated flexible heater (KH-408/5) was powered by a stabilized voltage source. The wattage of the heater is 10 W/in^2 , generating plates temperature higher than 80°C . For the calculations of heat transfer coefficient it was considered that the heater distributed the heat evenly to the plates. To isolate the experiment from external environmental changes, the experimental setup was placed into a natural convection chamber as shown in Fig. 6.

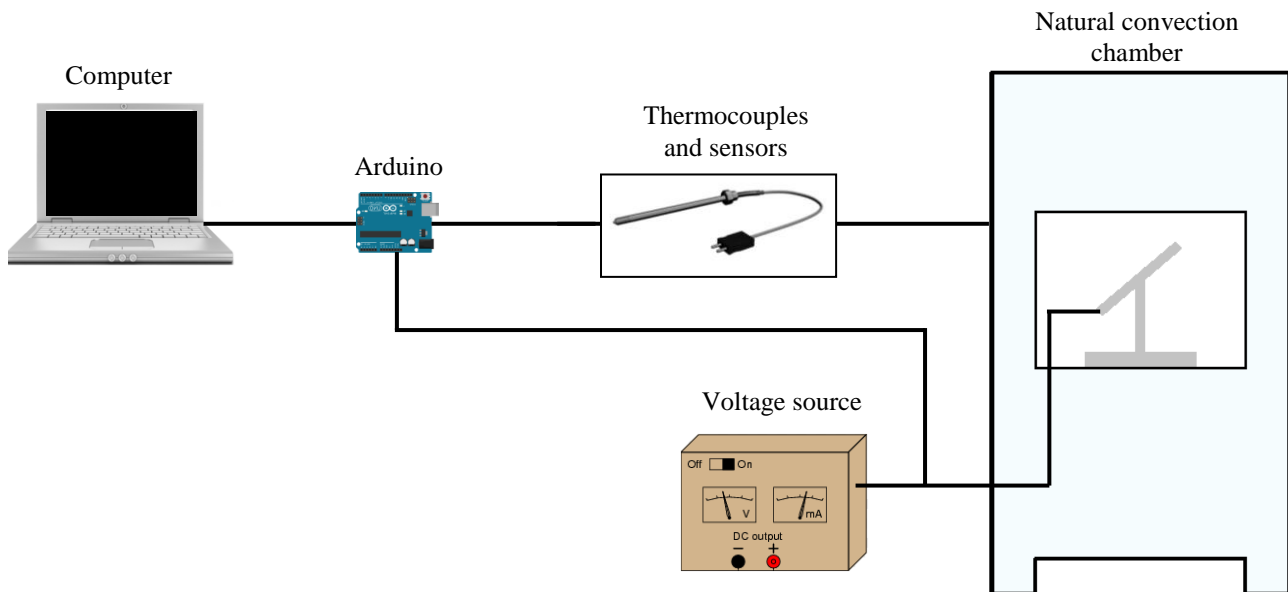


Figure 6: Schematic experimental apparatus.

The angle of inclination is set as -20° , -25° , -30° , -35° , -40° , -45° , -50° , -55° and -60° with respect to the horizontal position for each plate temperature. The stabilized voltage source was kept at $20 \pm 0,5\text{V}$ and $40 \pm 0,5\text{V}$. The data was obtained after the temperature stabilization when there was only variation due to the sensitivity of the sensors and heat transfer by natural convection. The \bar{h} for inclined plate surfaces was calculated using the plate-to-temperature difference data.

4. RESULTS AND DISCUSSION

The natural convection flow on a flat plate was characterized by an upward plume which forms as a consequence of the heated fluid near the plate surfaces. The boundary layer is formed on the surfaces of the plate and has unstable behavior influenced by the angle of inclination from horizontal (ϕ).

Figure 7(a) shows the temperature contour for the 3D inclined plate with $\phi = 10^\circ$ and $Ra = 6,72\text{E}+05$, located in a plane ZY on the plate. It is possible to observe the formation of vertical temperature plumes in the middle of the plate as

a consequence of the creation of hydrodynamic and thermal instabilities in the boundary layer. This provides a better heat transfer between the heated surfaces and the thermal boundary outer layer regions. The streamlines in the same plane are illustrated in Fig. 7(b), indicating the different effects of flow hydrodynamics.

The temperature contour and streamlines for the same plate for 2D flow do not have the formation of vertical plumes in the middle of the plate as shown in Fig. (8).

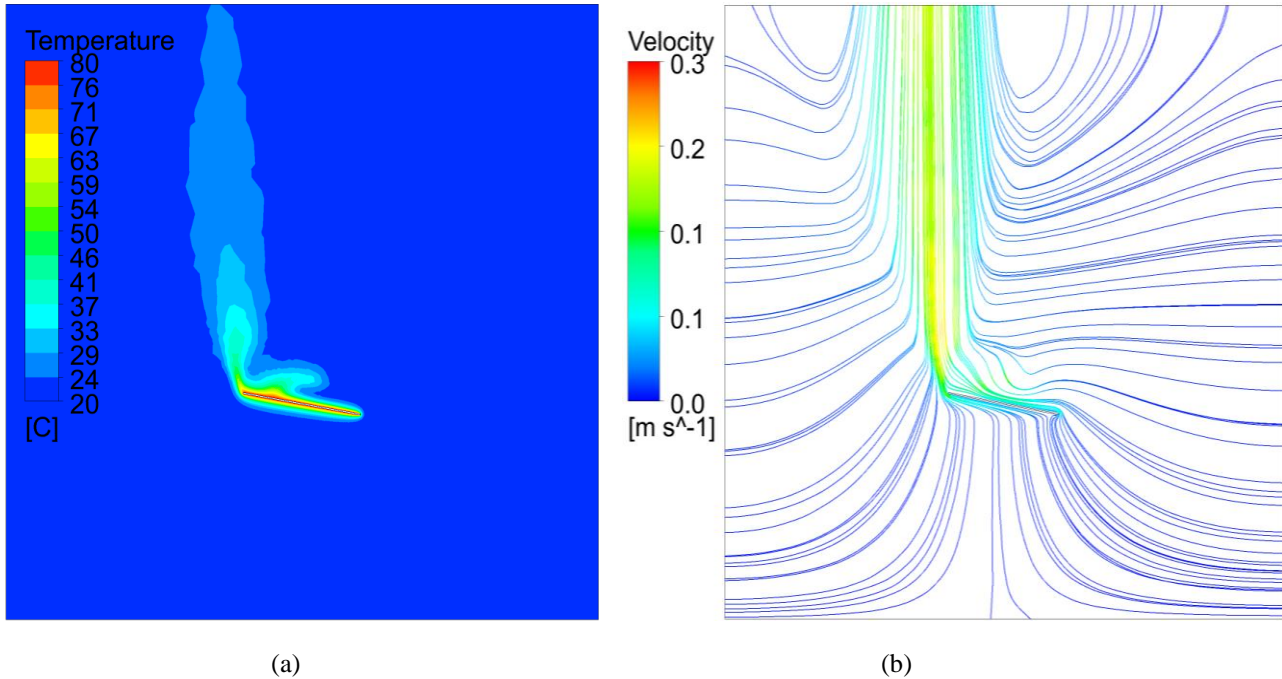


Figure 7: 3D inclined plate at 10° from the horizontal. (a) temperature contours; (b) velocity streamlines.

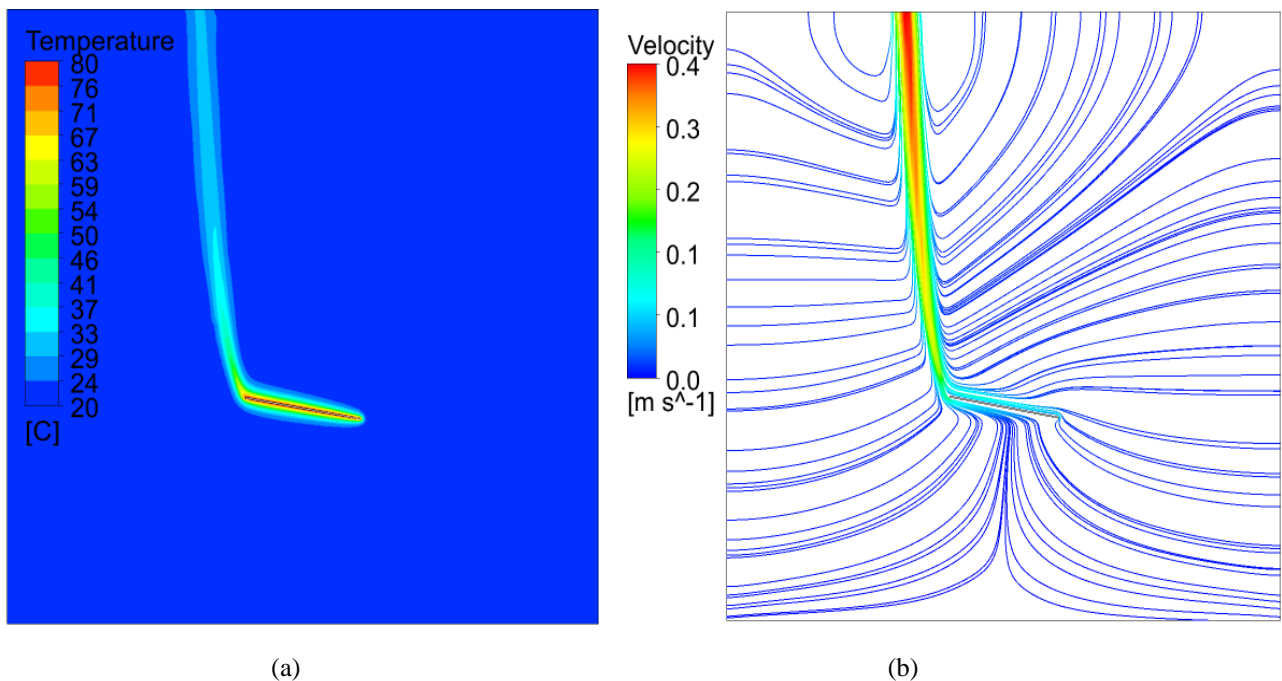


Figure 8: 2D inclined plate at 10° from the horizontal. (a) temperature contours; (b) velocity streamlines.

A reliable way to verify the influence of this phenomenon in the heat transfer of the plate is to compare \overline{Nu}_L obtained from the 2D and 3D plate surfaces. Figure 9 shows numerical results for both \overline{Nu}_L 2D and 3D inclined

plates from $Ra = 6,72E+05$ to $Ra = 3,36E+06$. It is possible to observe that 3D surfaces have a higher heat transfer coefficient than 2D surfaces due to the three-dimensional flow effects.

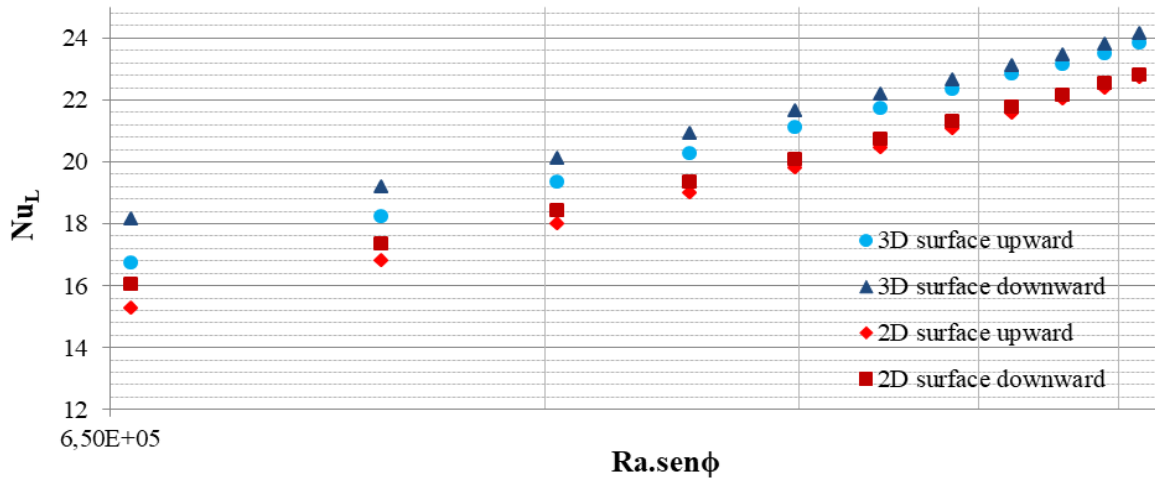


Figure 9: Inclined heated flat plate, $T_w = 80^\circ\text{C}$.

The larger is the ϕ value the smaller is the contribution of the 3D flow effects and the smaller is the creation of vertical plumes in the middle of the flat inclined plate. Figure 10 shows the temperature contour and streamlines for the 3D plate with $\phi = 60^\circ$ and $Ra = 3,36E+06$, located in the same plane as Fig. 7. It is possible to notice that there is no formation of plumes in the normal direction of the plate.

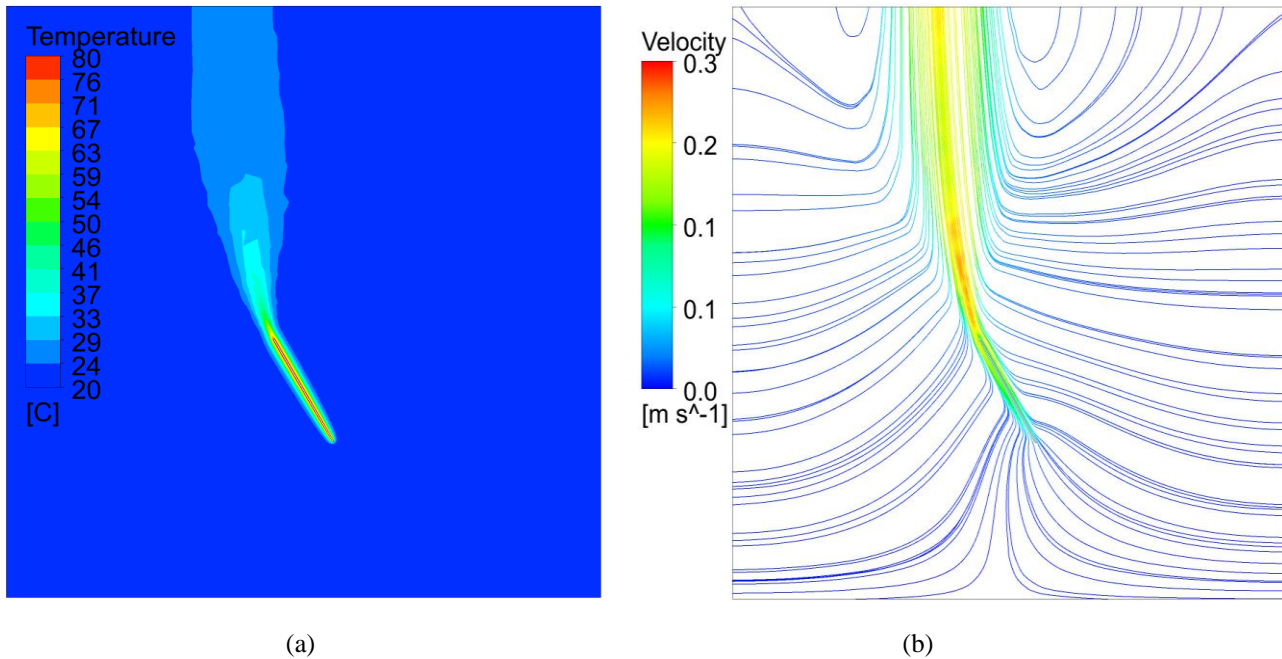


Figure 10: 3D inclined plate at 60° from the horizontal. (a) temperature contours; (b) velocity streamlines.

According to Vliet (1969) for the laminar regime, the solutions and correlations for a vertical plate may be used for a plate inclined at 30° to 90° from the horizontal, if the component of gravity parallel to the surface is used in the Rayleigh number. In this present work, as mentioned previously, the ϕ values less than 30° were simulated to verify this conclusion.

Comparison of the $\overline{Nu_L}$ for different $Ra \cdot \sin(\phi)$ for 2D and 3D flat inclined plate surfaces (upward and downward) obtained from numerical simulations, calculated from the Churchill and Chu's correlation and from the experimental results are shown in Fig. 11. The 2D and 3D numerical results agree well with the empirical correlation, with 2D presenting closer results. The $\overline{Nu_L}$ experimental shows better results with 3D numerical results, indicating the 3D flow effects influence in the heat transfer coefficient.

Good results were also obtained for angle of inclination smaller than 30° , demonstrating that the correlation for the vertical plate may be used for a plate inclined at 10° to 90° from the horizontal by varying the direction of g .

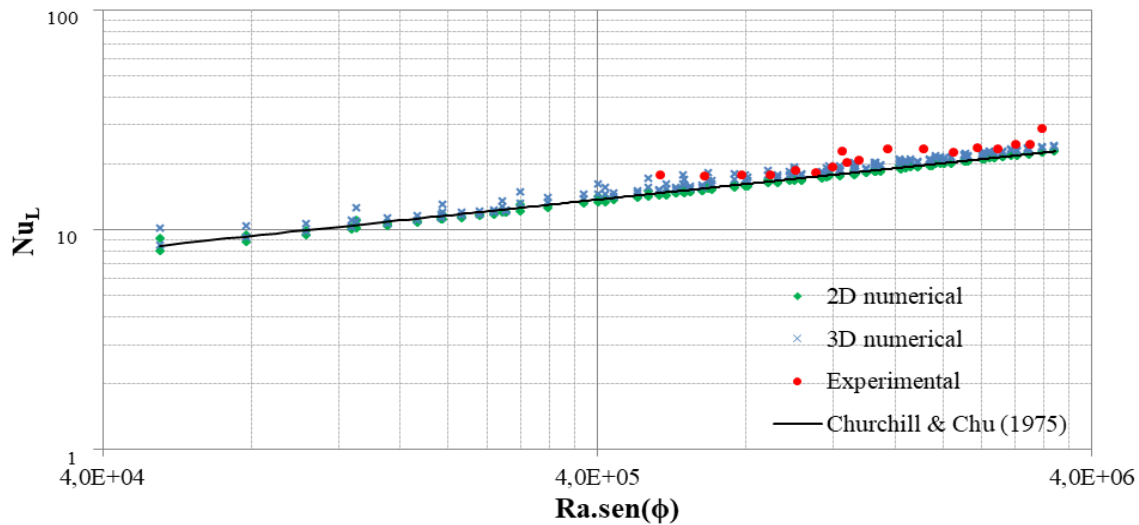


Figure 11: Inclined heated flat plate.

5. CONCLUSIONS

An appropriate numerical model approach was found. The results of this new approach agreed well with the experiment and available correlations. A steady-state natural convection heat transfer numerical study was performed for a laminar flow on flat inclined plates using a Boussinesq approximation. A vertical model was carried on to validate the modeling approach.

The average Nusselt numbers (\overline{Nu}_L) was obtained for both plate surfaces upward and downward for 2D and 3D simulations. The 3D results were slightly higher than 2D as consequence of 3D flow effects. A formation of vertical plumes in the middle of the upper face of the plate was obtained for 3D temperature contour. The smaller is the angle of inclination from horizontal (ϕ) the larger is the formation of the vertical plumes in the middle of the flat inclined plate.

The correlations for a laminar regime for a vertical plate may be used for a plate inclined at 10° to 90° from the horizontal if the component of gravity (g) parallel to the surface is used in the Rayleigh number (Ra).

6. REFERENCES

- Azevedo, L. F. A. and Sparrow, E. M., 1985. "Natural convection in open-ended inclined channels". *Journal of Heat Transfer*, Vol. 107, pp. 893-901.
- Churchill, S.W. and Chu, H.H.S., 1975. "Correlating equations for laminar and turbulent free convection from a vertical plate". *International Journal of Heat Mass Transfer*, Vol. 18, pp. 1323-1329.
- Fujii, T. and Imura, H., 1972. "Natural-convection heat transfer from a plate with arbitrary inclination". *International Journal Heat and Mass Transfer*, Vol. 15, pp. 755-767.
- Jubayer, C. M., Siddiqui, K. and Hangan, H., 2016. "CFD analysis of convective heat transfer from ground mounted solar panels". *Solar Energy*, Vol. 133, pp. 556-566.
- Pinheiro, L. A., Brasil Junior, A. P. and Silva, E. C. M., 2016. "Natural convection in photovoltaics panels". In *Proceedings of the 9th National Congress of Mechanical Engineering – CONEM2016*, Fortaleza, Brazil.
- Souza, A.D., Brasil, A.C.P.J. and Almeida, M.H.P., 1993. "Natural convection on flat and finite inclined plates". *Journal of the Brazilian Society of Mechanical Sciences*, Vol. 15, pp. 360-367.
- Tari, I. and Mehrtash, M., 2013. "Natural convection heat transfer from inclined plate-fin heat sinks". *International Journal of Heat and Mass Transfer*, Vol. 56, pp. 574-593.
- Vliet, G. C., 1969. "Natural convection local heat transfer on constant-heat-flux inclined surfaces". *Journal of Heat Transfer*, Vol. 91, pp. 511-516.

7. RESPONSIBILITY NOTICE

The authors are the only responsible for the printed material included in this paper.